Article

Preparation of Activated Carbon from Co-Pyrolysis Activation of Fly Ash and Biomass

Min Xie [1], Jian Cheng [2], Li Xu [3], Liwei Wang [4],*, Anqi Chen [4], Shuhui Zhang [4],* and Xiaohan Ren [4],*

1   Harbin Electric Academy of Science and Technology Co., Ltd., Harbin 150028, China
2   Harbin Electric International Company Limited, Harbin 150028, China
3   Anhui Special Equipment Inspection Institute, 45 Dalian Road, Hefei 230051, China
4   Institute of Thermal Science and Technology, Shandong University, Jinan 250061, China
*   Correspondence: wanglw1996@126.com (L.W.); 201720327@mail.sdu.edu.cn (S.Z.); renxh@sdu.edu.cn (X.R.)

Abstract: Fly ash from waste incineration and waste poplar bark from furniture manufacturing are domestic wastes. In this study, fly ash and poplar bark were used as raw materials to prepare activated carbon via carbonization, steam activation and reagent modification. The effects of the raw material mixing ratio, carbonization temperature, activator concentration and modifier concentration on the physicochemical properties of the semi-coke and activated carbon were investigated through experiments. The experiment showed that when the carbonization temperature was 300 °C, the steam concentration was 20%, the mixing ratio of the poplar bark and fly ash (B:F) was 5:1, and the modifier was 6% K_2CO_3 reagent and 9% $CaCl_2$. The prepared activated carbon had a better yield, specific surface area and pore structure, and had an abundant surface functional group structure. This paper points out the direction for the industrial directional production of activated carbon adsorbents with excellent physical and chemical properties, which has practical significance.

Keywords: fly ash; poplar bark; carbonization; pore structure; activated carbon

1. Introduction

In recent years, with the acceleration of urbanization, the amount of municipal waste generated has also increased. The main harmless treatment methods for municipal waste include sanitary landfill, incineration and composting [1], and waste incineration will produce a large amount of fly ash. Fly ash is a waste generated in the process of waste incineration, and its main components are oxides of metals such as silicon, aluminum, iron, calcium and magnesium [2]. Nowadays, the means of dealing with fly ash are relatively traditional and singular, the treatment process is cumbersome and the cost is high. Biomass is a general term for organic matter converted into photosynthesis under the catalysis of solar energy. Waste biomass mainly includes agricultural waste and forest waste [3], such as barley straw [4], oak [5] and rice husk [6], which are mainly composed of cellulose, hemicellulose and lignin. The world's poplar forests are rich in resources, and a large amount of poplar bark accumulates in warehouses, which will cause the risk of fire. At the same time, the combustion efficiency of poplar bark is low, and a large amount of polluting gases will be produced when burning [7]. Activated carbon is a porous material that is widely used in adsorption. It has the characteristics of cleanliness, high adsorption efficiency and reusability. It is widely used in industrial and living fields around the world [8]. Traditional activated carbon is usually prepared from carbonaceous materials, such as coal, pitch, petroleum and fruit stone, and is used as a precursor material for pyrolysis and activation. However, coal, petroleum and other materials are non-renewable and expensive to collect. In recent years, more and more attention has been paid to the research of activated carbon [5,9–11]. Using waste biomass and fly ash as raw materials to prepare activated carbon adsorbents has high research value regarding improving adsorption efficiency, saving resources and controlling environmental pollution [3,12–15].

The activation methods of activated carbon can be divided into three types: physical activation, chemical activation and physical–chemical activation [16–18]. During the physical activation, the carbonization process is carried out first, and then the activation process is carried out. Gas physical activation usually uses steam [19], CO_2 gas [20] or a mixture of the two [21] as the activator. The commonly used activators for chemical activation are KOH, NaOH, $ZnCl_2$, K_2CO_3 and H_3PO_4 solutions [22,23]. It is generally believed that the activation of CO_2 gas will promote the formation of the microporous structure of the activated carbon, while the activation of steam will mainly promote the formation of the mesoporous and macroporous structure of the activated carbon, thereby affecting the pore size distribution [7]. The adsorption performance of activated carbon is mainly affected by the specific surface area, pore structure and surface functional groups [24–26]. Figueiredo et al. [27] modified activated carbon via gas and liquid phase oxidation and explored the pyrolysis temperature of different oxygen-containing functional groups. It was found that the pyrolysis temperature should be controlled within an appropriate range. If the temperature is too high, the carbon content will decrease. If the temperature is too low, the pyrolysis will be incomplete and the pore formation will be insufficient. Thompson et al. [28] conducted activated carbon adsorption experiments in fields containing dichlorodiphenyltrichloroethane (DDT) and chlordane and found that the adsorption effect of activated carbon was affected by the particle size, and the pore volume and pore size distribution were also key elements that affected the adsorption performance of activated carbon. Wang et al. [24] used sludge and waste poplar bark as raw materials, activated them at 800 °C for 1 h, and found that both the mixing ratio of raw materials and the carbonization temperature affected the physicochemical properties and adsorption performance of activated carbon. Karanfil et al. [29] compared the adsorption capacity of two kinds of synthetic organic pollutants (trichloroethylene and trichlorobenzene) using coal-based and wood-based granular activated carbons. Micropores and steric hindrance effects were found to be physical factors that affected the adsorption of granular activated carbon. The adsorption performance of activated carbon is related to physical properties and depends on the chemical composition and chemical structure. Studies showed that the adsorption capacity of activated carbon prepared under high-temperature conditions is higher than that of activated carbon prepared under low-temperature conditions, mainly because the activated carbon prepared under high-temperature conditions has higher aromaticity and lower polarity [30].

Metal ions can also improve the adsorption properties of activated carbon. Activated carbon modification refers to improving the adsorption capacity by changing the physical structure or chemical properties of the activated carbon surface. The most common modification method is to use oxidizing or reducing agents to increase the abundance of functional groups on the surface of activated carbon. Commonly used oxidants are HNO_3, O_3, H_2O_2, etc. The most widely used oxidant is HNO_3 [31]. Strelko et al. [32] modified activated carbon with a nitric acid solution as the oxidant and found that the pore volume of the modified activated carbon decreased, the surface acidic functional groups increased and the activated carbon had a cation exchange capacity in a wider pH range. Liu et al. [33] used K_2CO_3 solution and NH_3 gas to modify the activated carbon to adsorb SO_2 and NO, and found that the activated carbon modified with NH_3 and K_2CO_3 solution promoted the synergistic adsorption of both SO_2 and NO. Wang et al. [34] used different concentrations of ammonia solution to modify activated carbon and found that the adsorption efficiency of activated carbon was the highest (68%) when the concentration of ammonia solution was 15% without heating modification. In order to better improve the adsorption performance of activated carbon, this study first explored the experimental conditions, such as the carbonization temperature, raw material mixing ratio and activator concentration, during the preparation of activated carbon. The composition of waste incineration fly ash was also analyzed, and K and Ca elements with a high content were explored. In the experiment, a solution containing K and Ca was selected to modify the activated carbon. In this paper, activated carbon was prepared via the co-carbonization, activation, and modification of

fly ash and waste poplar bark. It solved the problem of the high cost of activated carbon modifier and expanded the resource utilization channels of fly ash and waste poplar bark.

2. Materials and Methodology

2.1. Raw Materials and Pretreatment

In the experiment, fly ash from waste incineration in garbage factories and waste poplar bark from furniture manufacturing were selected as raw materials. The fly ash and poplar bark raw materials were put into a small pulverizer (800Y) for pulverization, and then the poplar bark with a particle size of 75–150 μm and fly ash with a particle size of 0–75 μm were screened out. The raw materials were placed in a constant temperature electric heating drying oven (101-OAB) at 105 °C for 18 h and then stored in a sealed container. Using an industrial analyzer (GYFX-3000) and elemental analyzer (Thermo Flash 2000) according to the GB/T212-2008 standard and GB/T28731-2012 standard, proximate analysis and ultimate analysis of raw materials were carried out, respectively. The proximate analysis and ultimate analysis data of the waste incineration fly ash and waste poplar bark are shown in Table 1. Table 2 shows several main elements of the waste incineration fly ash used in the experiment. It can be seen from Table 2 that the elements with the highest contents were Ca and K, which were much higher than the other metal elements.

Table 1. Proximate and ultimate analysis results of the raw materials.

Samples	Proximate Analysis (wt %) (ad)				Ultimate Analysis (wt %) (ad)				
	M	V	A	FC	C	H	S	N	O
Fly ash	1.00	7.84	87.3	3.88	0.830	1.25	6.24	0.05	91.6
Poplar bark	15.5	64.3	4.95	15.2	45.0	5.63	0.13	0.73	48.6

Note: M—moisture; V—volatile; A—ash; FC—fixed carbon; ad—air dry.

Table 2. Main metal element ingredients of the waste incineration fly ash.

Metal Element	ω (%)
Ca	14.37
K	9.62
Na	1.08
Al	0.72
Mg	0.71

2.2. Experimental System and Process

The experimental setup for activated carbon preparation is shown in Figure 1. The system consisted of three parts: a gas distribution system, a reaction system and a gas processing system. The gas distribution system included a N_2 tank, a steam generator and a connecting pipeline. The steam-generating device was composed of a micro-injection pump, a temperature control device and a heating cable. According to the demand flow of steam, after the conversion of the gas and liquid, the flow of liquid water was controlled by the program of the micro-injection pump. The temperature of the heating cable was kept stable at 110 °C using a temperature control device, thereby converting liquid water into gaseous water. The tubular horizontal heating furnace was mainly composed of a heating device, a temperature control device and a high-temperature-resistant quartz tube. The exhaust gas generated during the experiment was discharged after an exhaust gas treatment.

Before the experiment, the N_2 flow was adjusted to 500 mL/min and the high-temperature-resistant quartz tube was purged at room temperature to exhaust the air in the original quartz tube. The experiment was not started until the detected value of O_2 concentration at the outlet of the quartz tube was less than 0.05% to ensure that the carbonization experiment was carried out in an inert atmosphere. Then, the pretreated poplar bark and fly ash were weighed, mixed evenly and put into a high-temperature

crucible. The homogeneity test of the mixed sample was carried out to ensure the homogeneity of the sample. The switch of the high-temperature tubular reactor was turned on and the heating and cooling program of the experimental process was set. Since the reactor had a rated maximum heating rate, the heating rate was selected as 10 °C/min. A continuous flow of N_2 was maintained throughout the experiment, the sample was kept in an inert atmosphere in the tube and the crucible was taken out after the furnace tube was cooled to room temperature. The crucible containing semi-coke was weighed and recorded, and then put into a test tube, sealed and marked for inspection. In this study, the carbonization experiment was undertaken first, and through this preliminary analysis, the optimal mixing ratio of raw materials and carbonization temperature for carbonization were obtained. When studying the activation, this was used as a constant pre-carbonization condition, and experiments were carried out under different subsequent activation conditions. During the experiment, the temperature of the furnace tube was controlled by setting the temperature control program, and the activated carbon preparation conditions were changed by switching the carbonization and activation gases. The final data obtained in the experiment was the average value of three identical experiments.
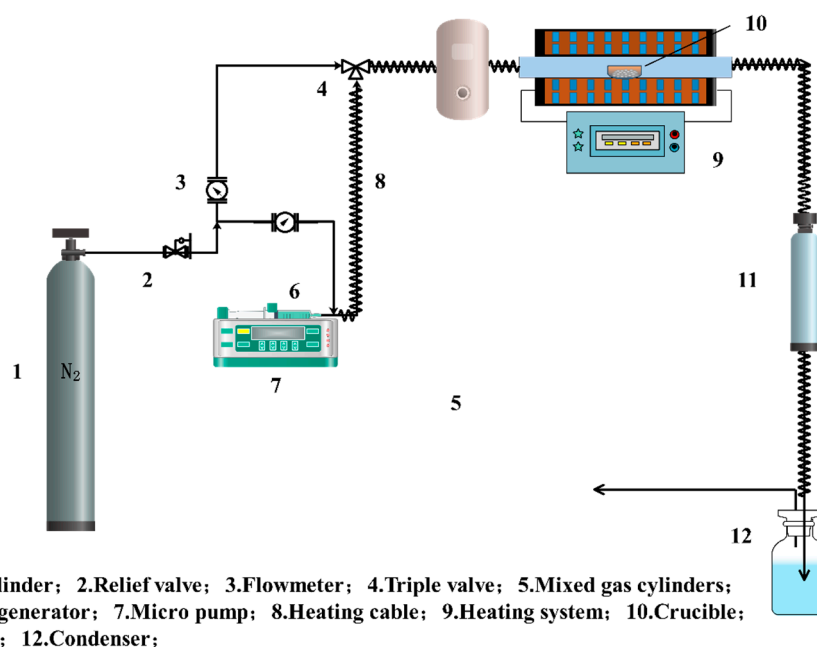

1.Gas cylinder；2.Relief valve；3.Flowmeter；4.Triple valve；5.Mixed gas cylinders；
6.Steam generator；7.Micro pump；8.Heating cable；9.Heating system；10.Crucible；
11.Filter；12.Condenser；

Figure 1. Schematic diagram of the experimental setup for the preparation of activated carbon.

2.3. Analysis and Characterization Methods

The semi-coke yield is the ratio of the carbonized product mass to the raw material mass, and the activated carbon yield is the ratio of the final weight to the initial raw material weight [8]. The "two-step activation method" was chosen for the experiment so that the yields could be calculated separately. The effect of adding fly ash to the preparation of activated carbon was more intuitively analyzed.

The BSD-PS4 series automatic specific surface and pore size analyzer produced by the Beijing Best Instrument Technology Co., Ltd. (Beijing, China), was used. Under ultra-low temperature conditions, the specific surface area of the sample was detected by using the principle that gas molecules have reversible adsorption properties on the surfaces of solid materials.

The surface morphology of the samples was observed using a SUPRA-55 field-emission scanning electron microscope (SEM) produced in Germany. By observing the surface structure and pore size of the samples, the theoretical analysis of the pore structure could be verified.

The types of functional groups on the surfaces of the samples were detected using the Nicolet iN10MX Fourier Transform Infrared Imaging Spectrometer (FTIR) produced by Thermo Fisher Scientific Co., Ltd. (Waltham, MA, USA).

3. Results and Discussion

3.1. Research on the Carbonization Process of Activated Carbon Preparation

The carbonization process mainly involves the cracking of macromolecules, the release of volatiles and the formation of preliminary pores. It is generally believed that raw materials with a high volatile content are more likely to form pore structures. From the industrial analysis results in Table 1, it can be known that the volatile matter content of poplar bark is as high as 64.3%. According to a previous study [35], it can be seen that the time required for the release of volatiles in the carbonization stage of biomass is relatively short, and a long carbonization time is not required. Excessive carbonization time will lead to the excessive ablation of carbon, resulting in excessive voids, and thus, a decrease in specific surface area. In the carbonization experiment, the carbonization time was selected as 30 min, and the effect of carbonization temperature and raw material mixing ratio on the semi-coke product was mainly studied. The total mass of each experimental sample was 6 g. The mixing ratios of poplar bark and fly ash (B:F) were 1:0, 2:1, 3:1, 4:1 and 5:1. The carbonization temperatures were 300 °C, 400 °C, 500 °C and 600 °C. The carbonization time was 30 min.

3.1.1. Effect of Carbonization Temperature and Raw Material Mixing Ratio on the Yield of Semi-Coke

Figure 2a shows the changing trend of semi-coke yield when the carbonization temperature was 300 °C, 400 °C, 500 °C and 600 °C. With the increase in carbonization temperature, the semi-coke yield showed a continuous downward trend. When the carbonization temperature increased from 300 °C to 400 °C, the semi-coke yield decreased significantly. In the temperature range of 300–600 °C, the decomposition reaction of raw materials occurred. In the temperature range of 300–400 °C, organic hydrogen bonds were broken, hydrogen and oxygen atoms were combined, macromolecules were cracked and water was volatilized. Each component underwent a violent depolymerization reaction, releasing a large amount of volatile matter [24–26]. In the range of 400–600 °C, the raw materials continued to be pyrolyzed by external heat, and the C-O bonds and C-H bonds were further broken to form C-C bonds. The volatiles were further released, the structure was aromatized and the fixed carbon content continued to increase. When B:F was 2:1, the carbonization temperature increased from 300 °C to 400 °C, and the semi-coke yield decreased by 15%, while from 500 °C to 600 °C, the semi-coke yield only decreased by 2.64%. This indicated that the release process of volatiles was mainly completed below 400 °C. When the carbonization temperature increased from 500 °C to 600 °C, a small amount of volatilization was found.

Figure 2b shows the variation trend of the semi-coke yield with the mixing ratio of raw materials. The raw material was pure biomass (B:F = 1:0) and was used as the control group. With the increase in the proportion of fly ash in the raw material, the semi-coke yield showed an upward trend at the same carbonization temperature. When the carbonization temperature was 500 °C, the semi-coke yield of the control group was 34.14%. When adding a small amount of fly ash (B:F = 5:1), the semi-coke yield increased significantly, and the difference in the semi-coke yield was due to the large difference in the volatile matter of the two raw materials. As can be seen from Table 1, the volatile matter content of poplar bark was 64.3%, while the fly ash was only 7.84%, which was a difference of nearly 9 times. Therefore, under the pyrolysis conditions at the same temperature, poplar bark released more volatiles. The higher the proportion of fly ash, the higher the semi-coke yield.
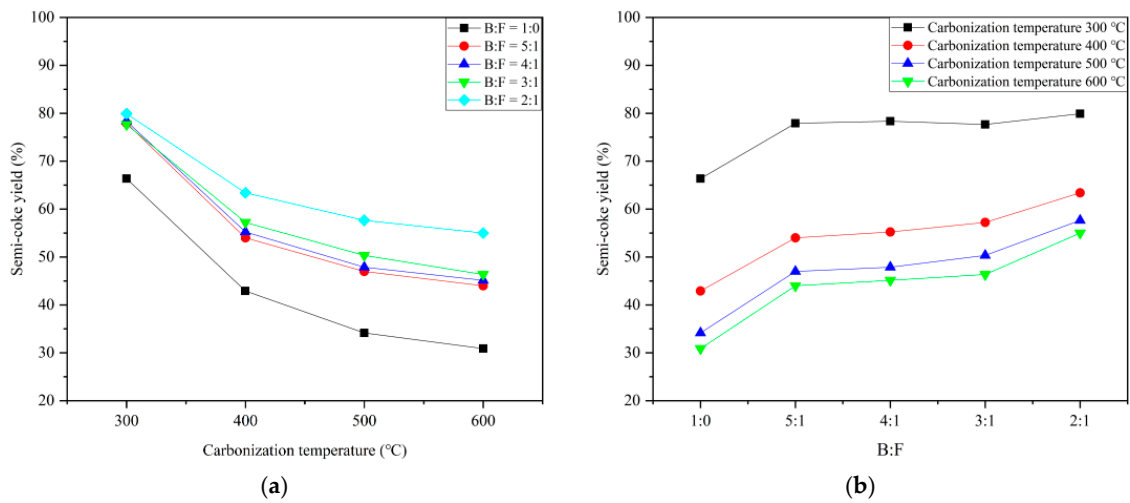
Figure 2. Variation trend of the yield of semi-coke with respect to the carbonization temperature and mixing ratio of raw materials: (**a**) different carbonization temperatures and (**b**) different mixing ratios of raw materials.

3.1.2. Effects of Carbonization Temperature and Raw Material Mixing Ratio on the Specific Surface Area of Semi-Coke

Figure 3a shows the variation trend of the specific surface area of semi-coke with carbonization temperature. Under the same mixing ratio of raw materials, the specific surface area of semi-coke prepared at a carbonization temperature of 500 °C and below was less than 15 m^2/g, which was much smaller than the specific surface area of semi-coke prepared at 600 °C. When the carbonization temperature increased from 500 °C to 600 °C, the specific surface area of semi-coke increased significantly. The reason was that when the carbonization temperature was 500 °C and below, the pyrolysis of the raw material was in progress and the pore-forming effect was poor. When the carbonization temperature rose to 600 °C, effectively all the volatile gases, such as H_2 and CH_4, in the biomass had been released, and a preliminary pore structure had been formed such that the specific surface area of the semi-coke increased significantly. When the carbonization temperature was 600 °C and B:F = 2:1, the specific surface area of the semi-coke reached the maximum value of 87 m^2/g.
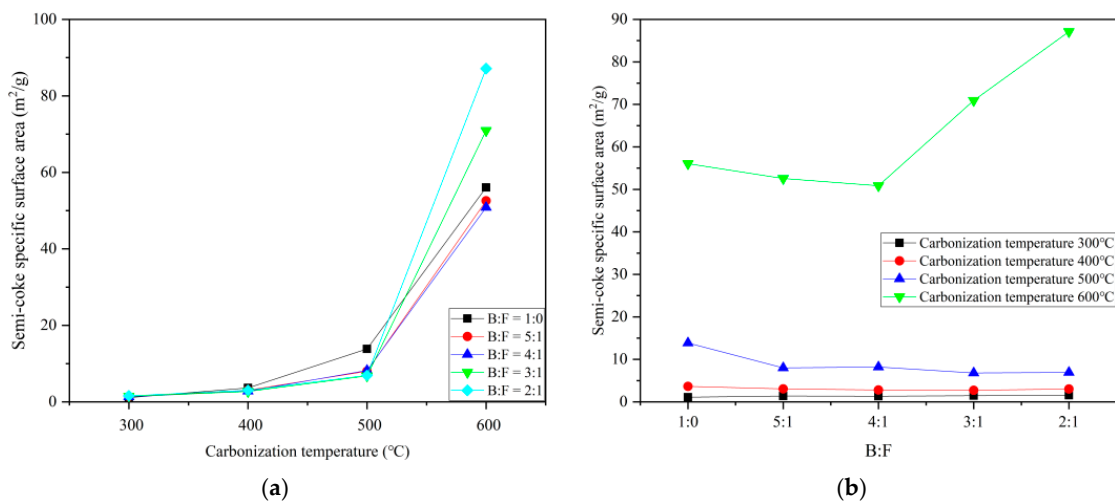

Figure 3. Variation trend of the specific surface area of semi-coke with respect to the carbonization temperature and mixing ratio of raw materials: (**a**) different carbonization temperatures and (**b**) different mixing ratios of raw materials.

It can be seen from Figure 3b that at lower carbonization temperatures (300 °C, 400 °C), the effect of the mixing ratio of raw materials on the specific surface area of semi-coke was small. At a lower temperature, the amount of volatile matter released by the raw material was relatively small, and the pore structures of the semi-coke were not very different for different mixing ratios, where all of the specific surface areas were small. When the carbonization temperature was 300 °C, the branched chains of hemicellulose, cellulose and lignin in the poplar bark were broken and thermally decomposed, and a large amount of volatile substances were released. At a temperature of 300 °C, the fly ash removed crystal water and released volatile matter, which provided H radicals, which were beneficial for the opening of closed pores in the poplar bark. When the carbonization temperature was 600 °C and the B:F increased from 4:1 to a larger value, the specific surface area of the semi-coke increased significantly. When the carbonization temperature was 600 °C, the process of releasing volatiles via the thermal decomposition of poplar bark had effectively been completed, and a preliminary pore structure had been formed. The fly ash was rich in metal ions, and the metal ions were adsorbed into the initial pore structure formed by the semi-coke such that the specific surface area of the semi-coke continued to increase.

3.2. Research on the Activation Process of Activated Carbon Preparation

It can be seen from the carbonization experiment that although the semi-coke product formed a preliminary pore structure, the specific surface area was still low, which is far from the standard for the industrial preparation of activated carbon. The semi-char product required further activation. By exploring the effects of carbonization temperature and raw material mixing ratio on semi-coke, the optimal carbonization conditions were determined (carbonization temperature of 300 °C; B:F of 2:1, 5:1 and control group 1:0). The activation temperature, activation time and activator concentration affect the physical and chemical properties of activated carbon. If a variety of reaction conditions are considered at the same time, it is difficult to determine the independent role of each factor. This study mainly explored the influence of the activation atmosphere.

The activation experiments were carried out in the same high-temperature horizontal tubular reactor setup as the carbonization experiments. After the carbonization process was over, there was no need to take out the intermediate product since we could directly adjust the gas and the temperature in the furnace and immediately enter the activation stage. The pre-mixed samples (B:F = 2:1, 5:1, 1:0) were carbonized at 300 °C for 30 min and then heated to 600 °C. Different concentrations of steam (0%, 5%, 10%, 15%, 20%, 25%) were used to activate the semi-coke. During the experiment, the total gas flow was set to 1000 mL/min, the flow of steam required in the activation stage was adjusted with a micro-syringe pump and the remainder was supplemented with N_2; then, activation took place at a temperature of 600 °C for 30 min.

3.2.1. The Effect of Steam Concentration and Raw Material Mixing Ratio on the Yield of Activated Carbon

Figure 4a shows the variation trend of the activated carbon yield with steam concentration. On the whole, the yield of activated carbon hardly changed with the change in steam concentration. Among the three different mixing ratios of raw materials, when the mixing ratio of raw materials was B:F = 2:1, the yield of activated carbon varied significantly with the concentration of steam. The higher the proportion of fly ash, the higher the activated carbon yield. When B:F = 2:1, the yield of activated carbon was 52%, and when B:F = 1:0, the yield of activated carbon was only 32%. Compared with the carbonization experiment, it can be seen that when B:F = 2:1, the carbonization temperature was 600 °C and the carbonization time was 30 min, the semi-coke yield was 53.19%. At the same temperature and the same mixing ratio of raw materials, the yield of activated carbon without activator activation was 52.63%, which was slightly lower than that of the semi-coke. This showed that with the continued extension of pyrolysis time, there was still a small amount of volatile matter precipitation in the inert atmosphere.
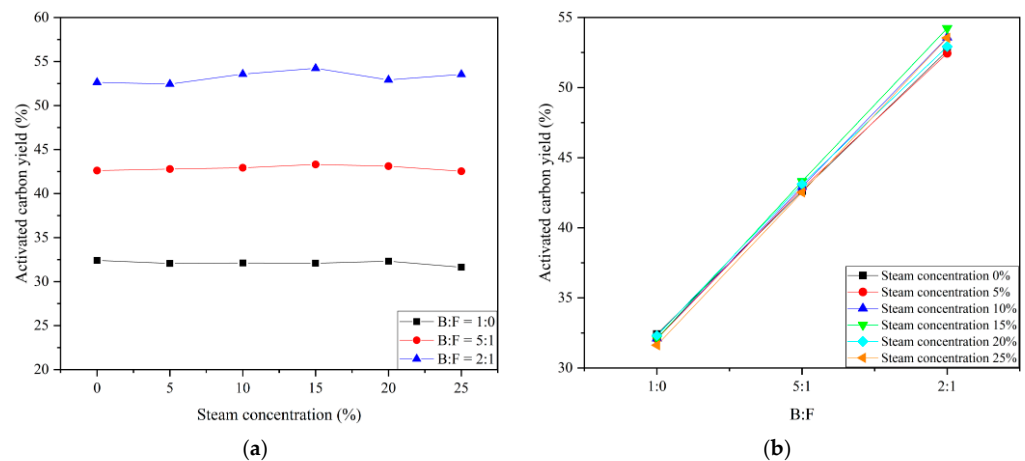
Figure 4. Variation trend of the yield of activated carbon with respect to the steam concentration and raw material mixing ratio: (**a**) different steam concentrations and (**b**) different mixing ratios of raw materials.

Figure 4b shows the variation trend of activated carbon yield with the mixing ratio of raw materials. The yield of activated carbon increased with the proportion of fly ash. When B:F = 1:0 (pure biomass was used as the raw material), the yields of activated carbon prepared via activation with different steam concentrations were all about 32%. When B:F = 2:1, the yield of activated carbon was about 53%. This phenomenon was similar to the yield change of semi-coke, which was mainly related to the difference in the volatile content of the two raw materials. The higher the mixing ratio of fly ash in the raw material, the higher the yield of activated carbon.

3.2.2. The Effect of Steam Concentration and Raw Material Mixing Ratio on the Specific Surface Area of Activated Carbon

Figure 5a shows the variation trend in the activated carbon-specific surface area with steam concentration. When there were no activators in the reaction, the specific surface area of the activated carbon prepared using B:F = 1:0 (pure biomass as raw material) was the largest. After adding the activator, the specific surface area of the activated carbon prepared from various raw materials increased to varying degrees, indicating that steam could effectively promote the pyrolysis of the biomass.
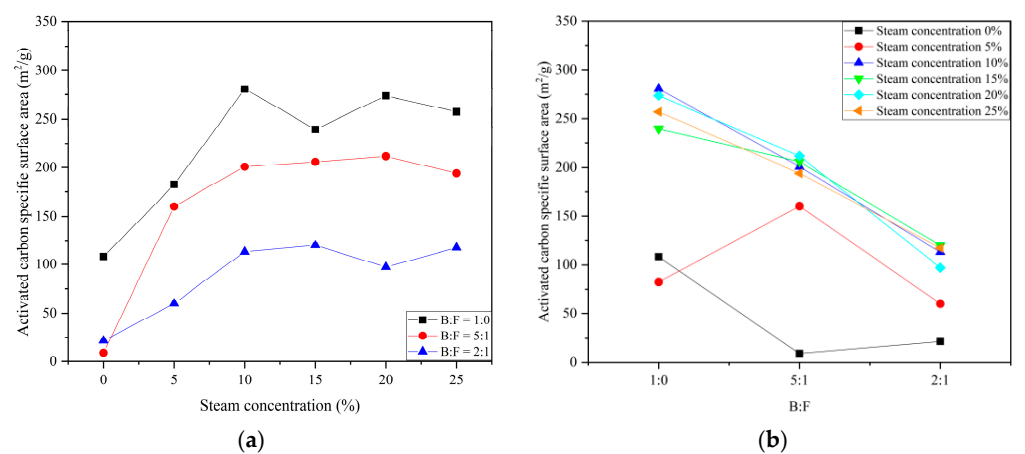

Figure 5. Variation trend of the specific surface area of activated carbon with respect to the steam concentration and raw material mixing ratio: (**a**) different steam concentrations and (**b**) different mixing ratios of raw materials.

It can be seen from Figure 5b that the specific surface area of activated carbon was the largest when the steam concentration was 5% and B:F = 5:1. This showed that in a suitable activation atmosphere, adding a small amount of fly ash into the raw material could improve the specific surface area of activated carbon. Regarding the mixing ratio of other raw materials, with the increase in fly ash content, the specific surface area of activated carbon showed a downward trend. When B:F = 2:1, the increase in the specific surface area of activated carbon was significantly smaller than that when B:F = 5:1. The specific surface area of the activated carbon prepared using B:F = 1:0 (that is, pure biomass as the raw material) was generally larger, and the specific surface area of the activated carbon prepared when B:F = 2:1 was generally smaller. This showed that when the fly ash was added in a large dose, it hindered the pyrolysis of biomass and reduced the specific surface area of the activated carbon.

3.2.3. Surface Morphology of Activated Carbon

It can be seen from Figure 6a that the surface of the activated carbon prepared with B:F = 1:0 (the raw material was pure biomass) had fewer voids. Figure 6b is the SEM image of activated carbon when B:F = 2:1. It can be seen that the pore structure on the surface of the activated carbon product increased. Since the metal ions contained in the fly ash could enter the pores of the activated carbon, the modification could enrich the pore structure. Figure 6c is the SEM image of activated carbon when B:F = 2:1. It can be seen from the figure that the pore structures of different regions of the activated carbon were quite different, and the amount of fly ash exceeded the carrying capacity of the pores of the activated carbon; therefore, the reaction was not sufficient. As a result, some parts of the activated carbon were rich in pore structure, and some parts were gray-white or aggregated. Comparing the images in Figure 6a–c, it can be seen that the raw material composition significantly affected the surface morphology and pore structure of the activated carbon. When a small amount of fly ash was added as the raw material, the surface morphology of the activated carbon was better.
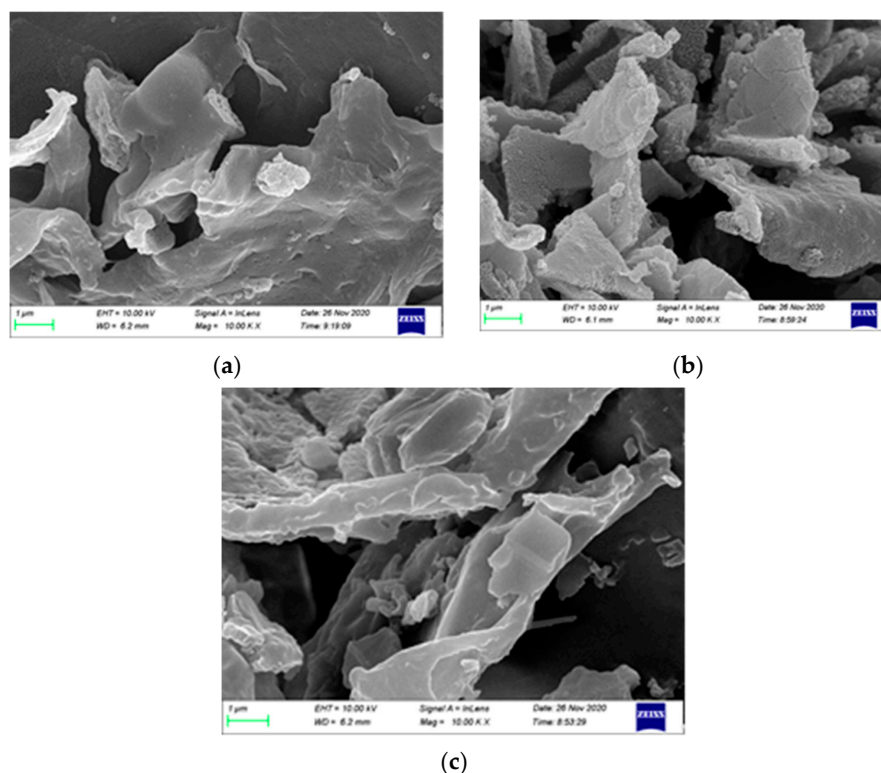

(a)

(b)

(c)

Figure 6. SEM images of activated carbon prepared using a 5% concentration of steam activation of raw materials with different mixing ratios: (**a**) B:F = 1:0, (**b**) B:F = 5:1 and (**c**) B:F = 2:1.

3.3. Effect of Adding Metal Compounds on the Preparation of Activated Carbon

Experiments showed that the incorporation of fly ash into poplar bark can improve the physical properties of activated carbon. Due to the complex composition and rich metal content of fly ash, the metal elements in fly ash may have an improvement effect on activated carbon because it conforms to the principle of loading material modification. It can be seen from Table 2 that the metal elements with higher contents in fly ash were K and Ca. In addition, the Cl element in fly ash was also relatively rich. Therefore, K_2CO_3 and $CaCl_2$ were selected in the experiment to explore their effects on the physicochemical properties of activated carbon.

The carbonization process and activation process in the modification experiments were the same as in the previous experiments, while the difference was the treatment of the raw materials. The required doses of K_2CO_3 and $CaCl_2$ in each group were weighed and fully dissolved in distilled water to prepare a modified solution. The ground and sieved poplar bark powder was weighed and placed in a crucible, the raw material was impregnated with the corresponding modification solution of each group and the solution was thoroughly stirred until it became a paste. The mixture was placed in a dry box and heated at 105 °C for 24 h. The fully impregnated and dried raw materials were put into a crucible and placed in a horizontal tubular reactor for carbonization and activation reactions. It can be seen from the activation experiment that the activation effect was the best when a small amount of fly ash was added to the raw material; therefore, we chose to use a low proportion of metal compounds for modification in this experiment. The ratios of modifiers (K_2CO_3 and $CaCl_2$) were 3%, 6%, 9% and 12% of the raw material mass. Three activation concentrations of steam, namely, 0%, 10% and 20%, were selected for activation exploration.

3.3.1. The effect of Adding K on the Yield and Specific Surface Area of Activated Carbon

It can be seen from Figure 7a that when the activator concentration was the same, the yield of activated carbon increased with the increase in the K_2CO_3 addition ratio. This showed that the addition of a small amount of K_2CO_3 could effectively improve the yield of activated carbon. When the K_2CO_3 addition ratio was the same, different activator concentrations could also affect the yield of activated carbon. The highest yield of activated carbon was obtained when the steam concentration was 10%. It can be seen that selecting the appropriate activator concentration and metal compound addition ratio could effectively improve the yield of activated carbon.
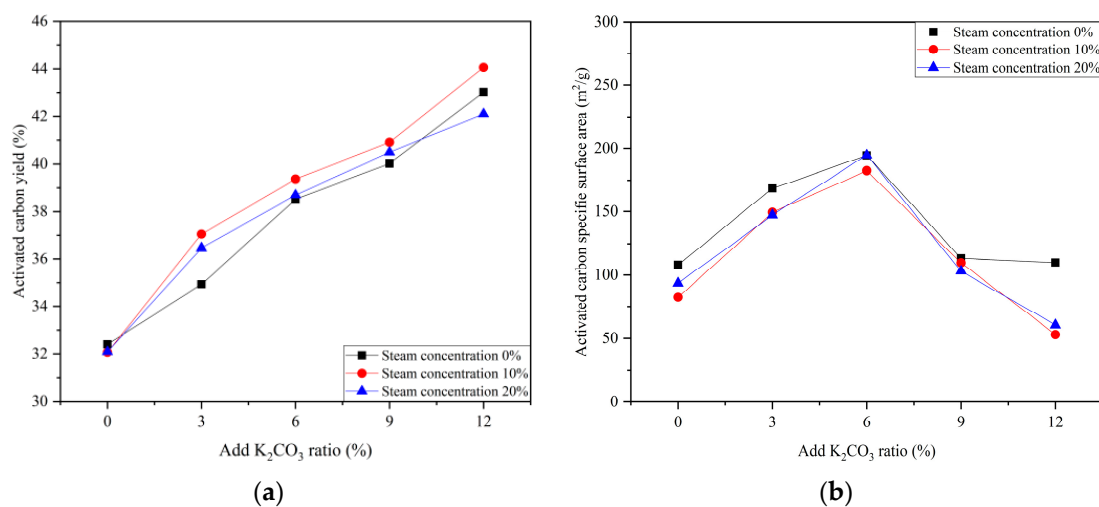

Figure 7. Variation trend of activated carbon yield and specific surface area with the addition ratio of K_2CO_3: (**a**) activated carbon yield and (**b**) activated carbon-specific surface area.

It can be seen from Figure 7b that under different steam concentrations, the changing trend of the specific surface area of activated carbon with the addition ratio of K_2CO_3 was

roughly the same. When the addition ratio of K_2CO_3 was 6%, the specific surface area of the obtained activated carbon product was the highest. Therefore, selecting an appropriate amount of added K could effectively increase the specific surface area of activated carbon.

3.3.2. The Effect of Adding Ca on the Yield and Specific Surface Area of Activated Carbon

It can be seen from Figure 8a that at the same activator concentration, the yield of activated carbon increased with the increase in the addition ratio of $CaCl_2$. When the steam concentration was 10%, the activated carbon yields were the highest under different $CaCl_2$ addition ratios. When the steam content was 20% and the $CaCl_2$ addition ratios were 9% and 12%, the yield of activated carbon was lower than that of activated carbon prepared in a gas-free activation atmosphere. It can be seen that when the additives are different metal compounds, it was necessary to select a suitable activation atmosphere and the addition ratio of the metal compounds so that the yield of the activated carbon could be higher. It can be seen from Figure 8b that when the steam concentration was 20%, the specific surface area of the activated carbon was the largest. Therefore, when the additive was $CaCl_2$, the activated carbon prepared with a higher steam concentration had a higher specific surface area. When the addition ratio of $CaCl_2$ was 9%, the specific surface area of the prepared activated carbon was the highest.
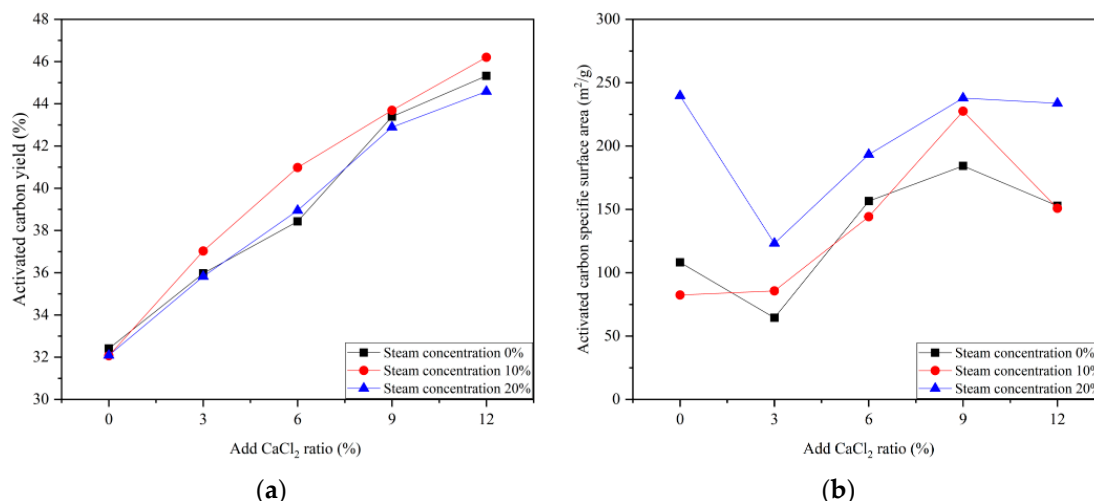

Figure 8. Variation trend of activated carbon yield and specific surface area with the addition ratio of $CaCl_2$: (**a**) activated carbon yield and (**b**) activated carbon-specific surface area.

3.3.3. Surface Morphology of Modified Activated Carbon

By comparing the SEM images of the activated carbon prepared using different concentrations of modifiers, it was found that the surface morphology and pore structure of the activated carbon were more abundant when modified using a 6% concentration of K_2CO_3 reagent and 9% concentration of $CaCl_2$ reagent. Figure 9a,b are the SEM images of activated carbon prepared via activation with 10% steam when the concentrations of 6% K_2CO_3 and 9% $CaCl_2$ were added to the biomass raw material, respectively. Figure 9a shows that when the modification concentration of K_2CO_3 was 6%, abundant pore structures could be observed, and the overall pore-forming effect was good. When the modification concentration of $CaCl_2$ was 9%, it can be seen from Figure 9b that the overall structure of the activated carbon was relatively uniform, which was beneficial to the pore formation of the activated carbon. Compared with the optimal modification concentration of K_2CO_3 of 6%, it was found that the activated carbon pores had different carrying capacities for different kinds of metal ions, and the optimal modification concentration of metal compounds was related to the concentration of cations.
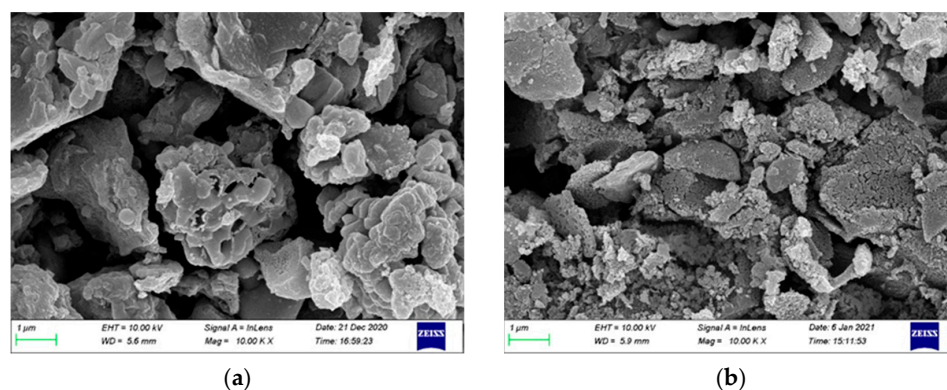
Figure 9. SEM image of activated carbon prepared using a 10% concentration steam activation when adding (**a**) 6% K_2CO_3 and (**b**) 9% $CaCl_2$.

3.3.4. Surface Functional Groups of Modified Activated Carbon

It can be seen from Figure 10 that the activated carbon modified using 6% K_2CO_3 and 9% $CaCl_2$ reagents had more absorption peaks in the wavenumber range of 4000–400 cm^{-1}. This shows that there were abundant surface functional groups in the activated carbons modified by the two reagents. Both modified activated carbons had significantly broad peaks around 3400 cm^{-1}, which were mainly formed by the stretching vibration of hydroxyl groups in alcohols, phenols and carboxylic acids [33,36]. Both activated carbons had continuous fluctuations in the wavenumber range of 2800–3000 cm^{-1}, which were formed by the saturated C-H stretching vibration. The absorption peak around the 2350 cm^{-1} wavenumber was considered to be formed by the vibration of accumulated double-bond functional groups, such as O=C=O. When the modified concentration of $CaCl_2$ was 9%, the prepared activated carbon had several peaks around the wavenumber of 1600–1400 cm^{-1}, which were mainly the peaks formed by the stretching vibration of the C=C functional group. The wavenumber range of 1300–1000 cm^{-1} is the stretching vibration region of C-O, indicating that both activated carbons contained this functional group. In the fingerprint region where the wave number was lower than 1000 cm^{-1}, the activated carbon modified with a 9% modified concentration of $CaCl_2$ contained obvious absorption peaks of aromatic hydrocarbons. However, the absorption peaks of activated carbon aromatic hydrocarbons modified by adding 6% K_2CO_3 were relatively weak, which was mainly related to the benzene ring substitution of aromatic polymers.
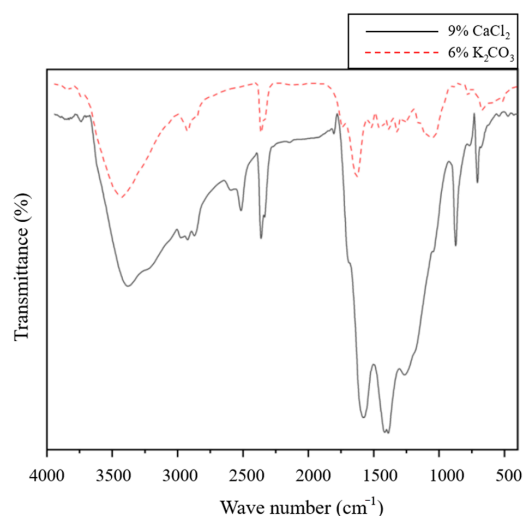

Figure 10. Fourier transform infrared absorption spectrum of activated carbon prepared by activation with a 10% concentration of steam when adding 6% K_2CO_3 and 9% $CaCl_2$.

4. Conclusions

Adding fly ash in the carbonization experiment could improve the yield and specific surface area of semi-coke to a certain extent. With the increase in carbonization temperature, the yield of semi-coke was inversely proportional to the specific surface area. The activation effect was the best when a small amount of fly ash was incorporated into the raw material. The yield of activated carbon was less affected by the concentration of the activator and more affected by the mixing ratio of the raw materials. The specific surface area and pore structure of activated carbon were greatly affected by the mixing ratio of raw materials and the concentration of the activator. Selecting the appropriate activator concentration and metal compound addition ratio could effectively improve the yield, specific surface area and pore structure of the activated carbon, and could improve the surface functional groups of activated carbon.

(1) With the increase in carbonization temperature, the yield of semi-coke gradually decreased, while the specific surface area of semi-coke gradually increased. When the carbonization temperature was 600 °C, the specific surface area of semi-coke was higher but the yield was lower. With the increase in the proportion of fly ash in the raw material, the yield of semi-coke showed an upward trend with little difference in specific surface area. When the mixing ratio of poplar bark and fly ash was 2:1, the specific surface area of semi-coke was greatly improved. When the carbonization temperature was 600 °C and B:F = 2:1, the specific surface area of semi-coke reached the maximum value of 87 m^2/g.

(2) The yield of activated carbon hardly changed with the concentration of steam but increased with the increase in the proportion of fly ash, which was mainly related to the content of volatile matter in the raw material. The larger specific surface area of activated carbon was concentrated in the range of a 10–20% steam concentration, and the activation process was limited when the steam concentration was too large or too small. In a suitable activation atmosphere, adding a small amount of fly ash into the raw material could improve the specific surface area and pore structure of activated carbon. When the carbonization temperature was 300 °C, B:F = 5:1 and a 20% concentration of steam was activated, the prepared activated carbon had an excellent specific surface area and pore structure.

(3) The yield, specific surface area and pore structure of activated carbon were better when modified with a 6% concentration of K_2CO_3 reagent and 9% concentration of $CaCl_2$ reagent. Through modification, a large number of surface functional groups can be introduced into the activated carbon, thereby improving the physical and chemical properties of the activated carbon.

Author Contributions: Investigation, writing—original draft preparation, M.X.; methodology, writing—original draft preparation, J.C.; data curation, L.X.; supervision, L.W.; writing—review and editing, A.C.; writing—original draft preparation, S.Z.; supervision, X.R. All authors have read and agreed to the published version of the manuscript.

Institutional Review Board Statement: Not applicable.

Informed Consent Statement: Not applicable.

Data Availability Statement: Not applicable.

Conflicts of Interest: The authors declare no conflict of interest.

References

1. Hadi, P.; Xu, M.; Ning, C.; Lin, C.S.K.; McKay, G.J.C.E.J. A critical review on preparation, characterization and utilization of sludge-derived activated carbons for wastewater treatment. *Chem. Eng. J.* **2015**, *260*, 895–906. [CrossRef]
2. Ahmaruzzaman, M.J.P. A review on the utilization of fly ash. *Prog. Energy Combust. Sci.* **2010**, *36*, 327–363. [CrossRef]
3. Zhang, T.; Walawender, W.P.; Fan, L.; Fan, M.; Daugaard, D.; Brown, R.J.C.E.J. Preparation of activated carbon from forest and agricultural residues through CO_2 activation. *Chem. Eng. J.* **2004**, *105*, 53–59. [CrossRef]
4. Pallarés, J.; González-Cencerrado, A.; Arauzo, I.J.B. Production and characterization of activated carbon from barley straw by physical activation with carbon dioxide and steam. *Biomass Bioenergy* **2018**, *115*, 64–73. [CrossRef]
5. Jung, S.-H.; Kim, J.-S.J.J. Production of biochars by intermediate pyrolysis and activated carbons from oak by three activation methods using CO_2. *J. Anal. Appl. Pyrolysis* **2014**, *107*, 116–122. [CrossRef]
6. Kalderis, D.; Bethanis, S.; Paraskeva, P.; Diamadopoulos, E. Production of activated carbon from bagasse and rice husk by a single-stage chemical activation method at low retention times. *Bioresour. Technol.* **2008**, *99*, 6809–6816. [CrossRef]
7. Ren, X.; Sun, R.; Meng, X.; Vorobiev, N.; Schiemann, M.; Levendis, Y.A. Carbon, sulfur and nitrogen oxide emissions from combustion of pulverized raw and torrefied biomass. *Fuel* **2017**, *188*, 310–323. [CrossRef]
8. Davini, P. SO_2 adsorption by activated carbons with various burnoffs obtained from a bituminous coal. *Carbon* **2001**, *39*, 1387–1393. [CrossRef]
9. Wang, X.; Zhu, N.; Yin, B.J. Preparation of sludge-based activated carbon and its application in dye wastewater treatment. *J. Hazard. Mater.* **2008**, *153*, 22–27. [CrossRef]
10. Tan, I.; Ahmad, A.; Hameed, B.J. Adsorption of basic dye on high-surface-area activated carbon prepared from coconut husk: Equilibrium, kinetic and thermodynamic studies. *J. Hazard. Mater.* **2008**, *154*, 337–346. [CrossRef]
11. Sekirifa, M.L.; Hadj-Mahammed, M.; Pallier, S.; Baameur, L.; Richard, D.; Al-Dujaili, A. Preparation and characterization of an activated carbon from a date stones variety by physical activation with carbon dioxide. *J. Anal. Appl. Pyrolysis* **2013**, *99*, 155–160. [CrossRef]
12. Ceyhan, A.A.; Şahin, Ö.; Baytar, O.; Saka, C. Surface and porous characterization of activated carbon prepared from pyrolysis of biomass by two-stage procedure at low activation temperature and it's the adsorption of iodine. *J. Anal. Appl. Pyrolysis* **2013**, *104*, 378–383. [CrossRef]
13. Xu, D.; Yang, L.; Ding, K.; Zhang, Y.; Gao, W.; Huang, Y.; Sun, H.; Hu, X.; Syed-Hassan, S.S.A.; Zhang, S.J.E.; et al. Mini-review on char catalysts for tar reforming during biomass gasification: The importance of char structure. *Energy Fuels* **2019**, *34*, 1219–1229. [CrossRef]
14. Danish, M.; Ahmad, T.J.R.; Reviews, S.E. A review on utilization of wood biomass as a sustainable precursor for activated carbon production and application. *Renew. Sustain. Energy Rev.* **2018**, *87*, 1–21. [CrossRef]
15. Li, Y.; Lu, L.; Lyu, S.; Xu, H.; Ren, X.; Levendis, Y.A.J. Activated coke preparation by physical activation of coal and biomass co-carbonized chars. *J. Anal. Appl. Pyrolysis* **2021**, *156*, 105137. [CrossRef]
16. Li, W.-H.; Yue, Q.-Y.; Gao, B.-Y.; Ma, Z.-H.; Li, Y.-J.; Zhao, H.-X. Preparation and utilization of sludge-based activated carbon for the adsorption of dyes from aqueous solutions. *Chem. Eng. J.* **2011**, *171*, 320–327. [CrossRef]
17. Hadi, P.; Gao, P.; Barford, J.P.; McKay, G.J. Novel application of the nonmetallic fraction of the recycled printed circuit boards as a toxic heavy metal adsorbent. *J. Hazard. Mater.* **2013**, *252*, 166–170. [CrossRef] [PubMed]
18. Xu, M.; Hadi, P.; Chen, G.; McKay, G.J. Removal of cadmium ions from wastewater using innovative electronic waste-derived material. *J. Hazard. Mater.* **2014**, *273*, 118–123. [CrossRef] [PubMed]
19. Nabais, J.M.V.; Nunes, P.; Carrott, P.J.; Carrott, M.M.L.R.; García, A.M.; Díaz-Díez, M. Production of activated carbons from coffee endocarp by CO_2 and steam activation. *Fuel Process. Technol.* **2008**, *89*, 262–268. [CrossRef]
20. Teng, H.; Lin, H.C. Activated carbon production from low ash subbituminous coal with CO_2 activation. *Fluid Mech. Transp. Phenom.* **1998**, *44*, 1170–1177. [CrossRef]
21. Zhu, Y.; Gao, J.; Li, Y.; Sun, F.; Gao, J.; Wu, S.; Qin, Y.J. Preparation of activated carbons for SO_2 adsorption by CO_2 and steam activation. *J. Taiwan Inst. Chem. Eng.* **2012**, *43*, 112–119. [CrossRef]
22. Abatan, O.G.; Oni, B.A.; Agboola, O.; Efevbokhan, V.; Abiodun, O.O.J. Production of activated carbon from African star apple seed husks, oil seed and whole seed for wastewater treatment. *J. Clean. Prod.* **2019**, *232*, 441–450. [CrossRef]
23. Kang, H.-Y.; Park, S.-S.; Rim, Y.-S.J.K. Preparation of activated carbon from paper mill sludge by KOH-activation. *Korean J. Chem. Eng.* **2006**, *23*, 948–953. [CrossRef]
24. Wang, L.; Lu, L.; Li, M.; Liu, Y.; Ren, X.; Levendis, Y.A.J. Effects of Carbonization on the Co-Activation of Sludge and Biomass to Produce Activated Coke. *J. Energy Resour. Technol.* **2021**, *143*, 102305. [CrossRef]
25. Wang, L.; Li, M.; Hao, M.; Liu, G.; Xu, S.; Chen, J.; Ren, X.; Levendis, Y.A. Effects of Activation Conditions on the Properties of Sludge-Based Activated Coke. *ACS Omega* **2021**, *6*, 22020–22032. [CrossRef]
26. Xu, S.; Li, M.; Li, Y.; Ren, X.; Zhu, W.; Levendis, Y.A.J. Preparation of Activated Coke by One-Step Activation Method, Ammonization, and K2CO3 Modification of Coal and Biomass. *J. Energy Resour. Technol.* **2022**, *144*, 012303. [CrossRef]
27. Figueiredo, J.L.; Pereira, M.; Freitas, M.; Orfao, J. Modification of the surface chemistry of activated carbons. *Carbon* **1999**, *37*, 1379–1389. [CrossRef]
28. Thompson, J.M.; Hsieh, C.-H.; Hoelen, T.P.; Weston, D.P.; Luthy, R.G. Measuring and modeling organochlorine pesticide response to activated carbon amendment in tidal sediment mesocosms. *Environ. Sci. Technol.* **2016**, *50*, 4769–4777. [CrossRef]

29. Karanfil, T.; Kilduff, J.E. Role of granular activated carbon surface chemistry on the adsorption of organic compounds. 1. Priority pollutants. *Environ. Sci. Technol.* **1999**, *33*, 3217–3224. [CrossRef]

30. Ahmad, M.; Lee, S.S.; Dou, X.; Mohan, D.; Sung, J.-K.; Yang, J.E.; Ok, Y.S. Effects of pyrolysis temperature on soybean stover-and peanut shell-derived biochar properties and TCE adsorption in water. *Bioresour. Technol.* **2012**, *118*, 536–544. [CrossRef]

31. Likodimos, V.; Steriotis, T.A.; Papageorgiou, S.K.; Romanos, G.E.; Marques, R.R.; Rocha, R.P.; Faria, J.L.; Pereira, M.F.; Figueiredo, J.L.; Silva, A.M.J.C. Controlled surface functionalization of multiwall carbon nanotubes by HNO_3 hydrothermal oxidation. *Carbon* **2014**, *69*, 311–326. [CrossRef]

32. Strelko Jr, V.; Malik, D.J.J. Characterization and metal sorptive properties of oxidized active carbon. *J. Colloid Interface Sci.* **2002**, *250*, 213–220. [CrossRef] [PubMed]

33. Liu, G.; Wang, L.; Li, Y.; Ren, X. Biomass and Coal Modification to Prepare Activated Coke for Desulfurization and Denitrification. *Energies* **2022**, *15*, 2904. [CrossRef]

34. Wang, L.; Sha, L.; Zhang, S.; Cao, F.; Ren, X.; Levendis, Y.A. Preparation of activated coke by carbonization, activation, ammonization and thermal treatment of sewage sludge and waste biomass for SO_2 absorption applications. *Fuel Process. Technol.* **2022**, *231*, 107233. [CrossRef]

35. Pena, J.; Villot, A.; Gerente, C. Pyrolysis chars and physically activated carbons prepared from buckwheat husks for catalytic purification of syngas. *Biomass Bioenergy* **2020**, *132*, 105435. [CrossRef]

36. Lee, D.Y.; Cho, J.-E.; Cho, N.-I.; Lee, M.-H.; Lee, S.-J.; Kim, B.-Y. Characterization of electrospun aluminum-doped zinc oxide nanofibers. *Thin Solid Film.* **2008**, *517*, 1262–1267. [CrossRef]